

Photogeneration and reactivity of flavin anionic semiquinone in a bifurcating electron transfer flavoprotein

H. Diessel Duan^{1†}, Sharique A. Khan¹ and Anne-Frances Miller^{1*}

¹Department of Chemistry, University of Kentucky, Lexington, KY 40506

Running title: Photogeneration of a bifurcating flavin semiquinone

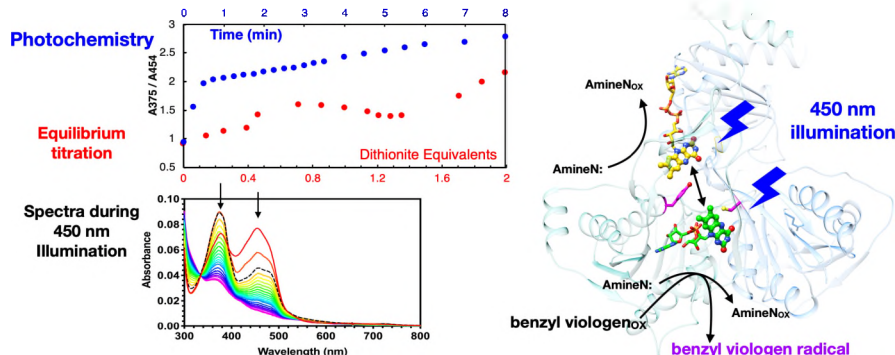
*To whom correspondence should be addressed: Anne-Frances Miller, Department of Chemistry, University of Kentucky, Lexington KY 40506-0055 U.S.A. Tel (859) 257-9349, Email afmill3r2@gmail.com Tel# (859) 257-9349.

† Current address Van Andel Institute, 333 Bostwick Ave. NE, Grand Rapids, MI, 49503, U.S.A.

Abstract

Electron transfer bifurcation allows production of a strongly reducing carrier at the expense of a weaker one, by redistributing energy among a pair of electrons. Thus, two weakly-reducing electrons from NADH are consumed to produce a strongly reducing ferredoxin or flavodoxin, paid for by reduction of an oxidizing acceptor. The prevailing mechanism calls for participation of a strongly reducing flavin semiquinone which has been difficult to observe with site-certainly in multi-flavin systems. Using blue light (450 nm) to photoexcite the flavins of bifurcating electron transfer flavoprotein (ETF), we demonstrate accumulation of anionic flavin semiquinone in excess of what is observed in equilibrium titrations, and establish its ability to reduce the low-potential electron acceptor benzyl viologen. This must occur at the bifurcating flavin because the midpoint potentials of the electron transfer (ET) flavin are not sufficiently negative. We show that bis-tris propane buffer is an effective electron donor to the flavin photoreduction, but that if the system is prepared with the ET flavin chemically reduced, so that only the bifurcating flavin is oxidized and photochemically active, flavin anionic semiquinone is formed more rapidly. Thus, excited bifurcating flavin is able to draw on an electron stored at the ET flavin. Flavin semiquinone photogenerated at the bifurcation site must therefore be accompanied by additional semiquinone formation by oxidation of the ET flavin. Consistent with the expected instability of bifurcating flavin semiquinone, it subsides immediately upon cessation of illumination. However comparison with yields of semiquinone in equilibrium titrations suggest that during continuous illumination at pH 9 a steady state population of 0.3 equivalents of bifurcating flavin semiquinone accumulates, and then undergoes further photoreduction to the hydroquinone. Although transient, the population of bifurcating flavin semiquinone explains the system's ability to conduct light-driven electron transfer from bis-tris propane to benzyl viologen, in effect trapping energy from light.

Graphical Abstract



Key Words Flavin, Photochemistry, Electron transfer, Electron bifurcation, Electron transfer flavoprotein

Introduction

Flavin-based electron bifurcation not only enables microorganisms to live at the thermodynamic limit [1, 2], but also addresses our urgent need to maximize the efficiency with which humanity utilizes energy. By coupling exergonic and endergonic electron transfers, electron bifurcation permits redistribution of energy among electrons to generate a more strongly reducing electron at the expense of the energy of the other electron of the original pair [3, 4]. Thus, reduced ferredoxin (Fd, reduction midpoint potential $E^\circ \approx -420$ mV) can be produced from NADH ($E^\circ \approx -320$ mV) by coupling this endergonic reaction to reduction of crotonyl-CoA to butyryl-CoA ($E^\circ \approx -10$ mV) as $2\text{Fd}_{\text{ox}} + 2 \text{NADH} + \text{crotonyl-CoA} \rightarrow 2\text{Fd}_{\text{red}} + 2 \text{NAD}^+ + \text{butyryl-CoA}$ [5].

In the best-characterized exemplars of NAD(P)H-based electron bifurcation, a flavin accepts the pair of electrons from NAD(P)H, and we call it the bifurcating flavin, Bf-flavin [2, 4, 6-8]. Of each pair, one electron is directed to Fd, sometimes via Fe₄S₄ clusters built-into the enzyme [9], whereas the other electron passes to a high- E° acceptor via a separate sequence of cofactors that incorporates a mechanism to enable only a single electron per pair to employ this path. In the bifurcating electron transfer flavoproteins (Bf-ETFs, Figure 1), a second flavin is the immediate high- E° electron acceptor, the so-called 'electron transfer' flavin or ET-flavin [10-13].

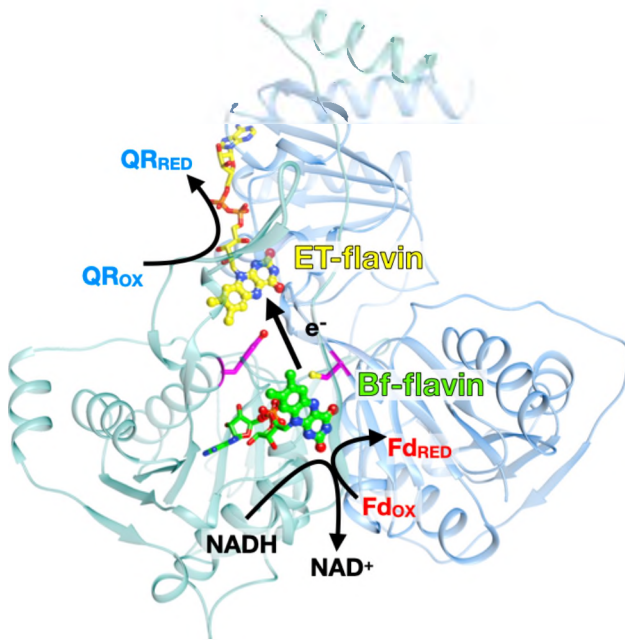


Figure 1. Ribbon diagram of the *RpaETF*, modeled onto the Bf-ETF of *Acidaminococcus fermentans* (4KPU.pdb [10]). This cartoon depicts the high- E° electron acceptor of *RpaETF* as 'QR' for quinone reductase, and the low- E° acceptor Fd, as well as the pairwise electron donor NADH. *RpaETF*'s two flavins are shown as ball-and-stick models, as well as the Tyr37.S and Cys174.L that we addressed in our mutagenesis, in pink (Tyr37.S between the flavins, Cys174.L above and to the right of the Bf-flavin).

Black arrows indicate chemical transformations as well as electron transfer between flavins.

Transfer of one electron from the doubly-reduced hydroquinone (HQ) state of the Bf-flavin to the ET-flavin must generate a semiquinone (SQ) state of the Bf-flavin. Crucially, this is understood to be a high-energy state embodying much of the energy of both electrons, and a key mechanistic intermediate in flavin-based bifurcating enzymes [14]. It is thought to react immediately or even in concert with its formation and thus to have the status of a transition state that participates mechanistically but is not

populated at thermodynamic equilibrium [9]. Indeed, transient absorption spectroscopy (TAS)¹ revealed lifetimes of photogenerated flavin anionic semiquinone (ASQ) attributed to the Bf-flavin ranging from 14 to 380 ps [9, 11, 15-17]. Because the flavin-based bifurcating systems studied so far by TAS contained more than one flavin, it was difficult to attribute spectral transients to a specific flavin. Moreover, a short-lived ASQ does not suffice to produce electron bifurcating activity [16]. Whilst both electron propagation and recombination can result in a short-lived ASQ, only charge propagation advances net reaction. To know which is occurring, it is desirable to be able to monitor signatures of electron propagation directly, for example via the distinct spectrum of a terminal acceptor, and to be able to modulate at least one of the two processes, for example by poising the system, as we describe below.

The photochemistry of flavins can provide invaluable insights into the mechanisms of flavoproteins [18, 19]. Oxidized (OX) flavins absorb blue light and this capacity is central to a variety of flavins' biological functions such as DNA repair, entrainment of circadian rhythm, phototropism, phototaxis, regulation of photosynthesis, stress responses, and more [20-26]. The inherent photoreactivity of flavins is realized in enzymes with no known photoreceptor function [27] and is exploited in common laboratory practice, wherein photoexcited flavin or deazaflavin is used as an aggressive reductant, and regenerated at the expense of a sacrificial electron donor such as ethylenediaminetetraacetic acid (EDTA) [28, 29].

Herein, we report analogous use of the buffer bis-tris propane (BTP) to supply reducing equivalents for flavin reduction upon blue light illumination, preventing the photodegradation documented for flavin alone [30, 31]. Moreover protective electron transfer from BTP permitted accumulation of ASQ attributable in part to the Bf-flavin in the Bf-ETF from *Rhodopseudomonas palustris* (*Rpa*ETF, also known as FixAB due to its association with nitrogen-fixation [17, 32, 33]). The photogenerated ASQ of *Rpa*ETF's Bf-flavin was previously described by TAS as a short-lived species with a half-life of 380 ps [15]. However *Rpa*ETF contains a second flavin, so distinguishing between the two is delicate. Whereas the Bf-flavin has an unstable ASQ, the ASQ of the ET-flavin is stable over a range of reduction potentials from -47 mV to -203 mV at pH 9 [15].

While the current study does not attain the time resolution required to elucidate kinetics and intermediates of electron transfer [34, 35], we were able to accumulate steady-state populations of photoreduced flavins that could represent states involved in turnover. The effects of replacing electron-rich amino acid side chains were minor, but demonstrate that our observations reflect protein-bound flavin. We provide evidence of both electron transfer between the two flavins in *Rpa*ETF, and electron transfer from photogenerated ASQ to an electron acceptor with an E° too low to be reducible by the ET-flavin [36], that therefore indicates the participation of Bf-flavin ASQ. Indeed, the stoichiometry with which ASQ accumulates exceeds what can be explained by the ET flavin alone, and therefore appears to include a contribution from the Bf-flavin. The photochemistry of *Rpa*ETF opens new avenues for exploring mechanisms by which bifurcating flavoenzymes execute this extremely ancient yet efficient energy-conserving strategy.

Results

Whereas TAS provides a view of what intermediates form and how they evolve as electrons move within the system, continuous illumination can reveal where reducing equivalents accumulate. Advantages include ability to draw on external reductants, while exploiting light's selective excitation of targets able to absorb the wavelengths chosen, and the fact that photons fundamentally drive one-electron processes. Photoexcited flavins are understood to acquire electrons from near-by amino acids [37-39], or

¹ Abbreviations: ASQ, anionic semiquinone; Bf, Bf-ETF, bifurcating electron transfer flavoprotein; Bf-flavin, bifurcating flavin; BTP, 1,3-bis(tris(hydroxymethyl)methylamino)propane, aka bis-tris propane; BV, benzyl viologen; EDTA, ethylenediaminetetraacetic acid; ETF, electron transfer flavoprotein; ET-flavin, electron transfer flavin; HQ, hydroquinone (fully reduced); NOX, NADH oxidase; NfnI, NADH-dependent reduced ferredoxin:NADP⁺ oxidoreductase; OX, oxidized; *Rpa*ETF, *Rhodopseudomonas palustris* ETF; TAS, transient absorption spectroscopy; Tris, tris(hydroxymethyl)aminomethane; WT, wild-type.

sacrificial electron donors provided in the solution [29, 40]. The latter strategy has been employed to maximize ASQ generation in several flavoenzymes [41, 42] where subsequent electron transfers to form HQ were slower [43]. Since the ASQ of the Bf-flavin is a critical mechanistic element of flavin-based bifurcation, we tested photoreduction in the presence of a sacrificial electron donor as a possible method for accumulating the elusive Bf-ASQ.

Bis-tris propane supplies reducing equivalents and prevents photodegradation of the flavins. – EDTA and deprotonated amines have commonly been used as a sacrificial electron donors [28, 29, 40]. Our system includes an efficient electron-donating amine in the guise of our buffer: bis-tris propane (BTP). In contrast to the photo-driven degradation observed in the absence of buffer (Figure 2A), full reduction of FAD is observed in our 20 mM pH 9.0 BTP buffer (Figure 2B). The integrity of the photoreduced FAD was confirmed by allowing it to reoxidize upon exposure to air, which restored the starting spectrum with no detectable alteration in spectral shape or amplitude (compare Fig. 2B blue and black curves). Once formed, flavin HQ is presumably immune to photodegradation in blue light due to its low absorption at 450 nm, and photoreduction was complete in half a minute resulting in little exposure overall (Fig. 2B). When Tris buffer was used instead of BTP, flavin reduction was 5-fold slower and only 76% of the flavin was recovered upon re-oxidation, with the rest apparently converted to lumichrome (Fig. 2C). In water, nearly 100% of FAD was converted to lumichrome, as has been demonstrated for FMN as well (Fig. 2A and [44]). Thus our pH 9 BTP buffer allows net redox chemistry to outpace irreversible covalent transformation of the flavin.

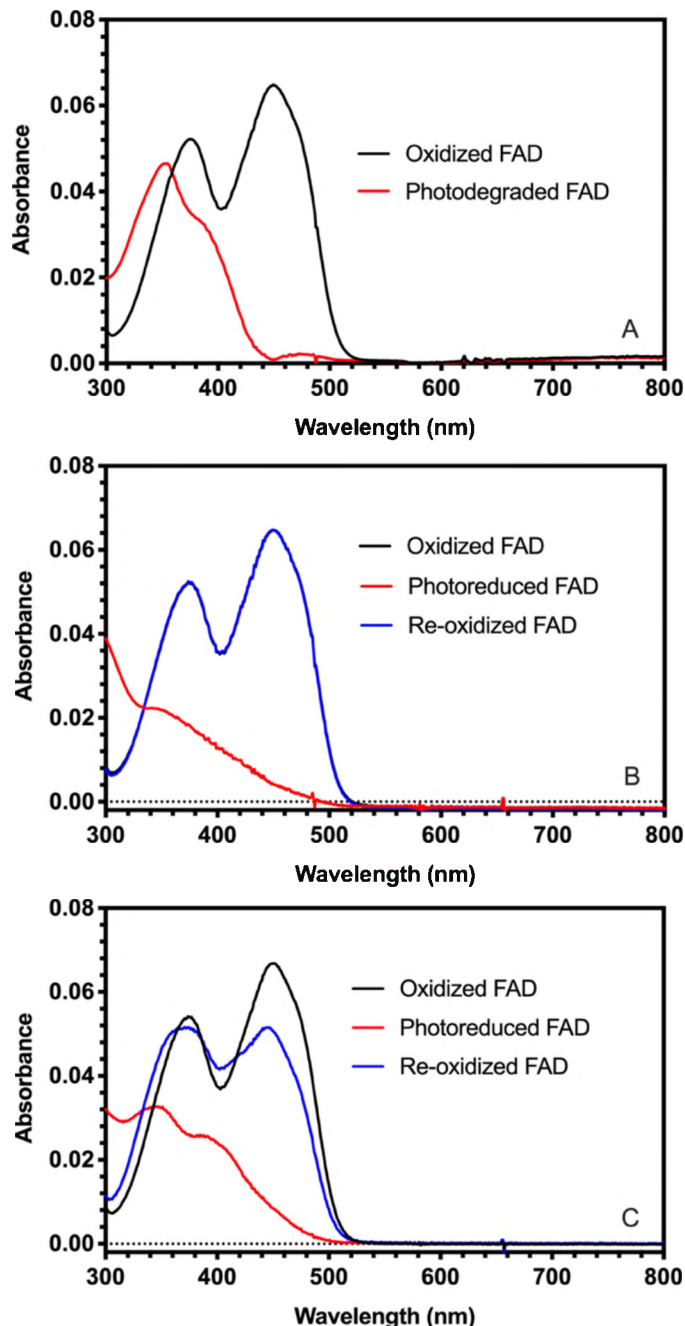


Figure 2. Photoreduction and re-oxidation (when possible) of 29.29 μ M FAD (A) illuminated in pure water, (B) illuminated for 0.5 min in 20 mM BTP, pH 9.0, 200 mM KCl, 10% (w/v) glycerol, and (C) illuminated for 2.5 min in 20 mM Tris, pH 9.0, 200 mM KCl, 10% (w/v) glycerol. In panel C, modification of the flavin manifests as a lower intensity at band I (445 nm) and a blue-shift of band II (near 375 nm) after photoreduction and recovery. Note that both blue and black traces are present in panel B, but are almost identical, indicating no modification of the flavin.

Photoproduction of flavin semiquinone in RpaETF – When WT RpaETF was illuminated with 450 nm light, we also observed full photoreduction of the bound flavins. However the process was both slower and different, as we observed formation and then consumption of ASQ during illumination, whereas no

radical intermediates were observed for the free FAD in Tris buffer (Figure 3). Indeed, Figure 3A shows that free FAD undergoes a homogeneous reduction to HQ with a well-defined isosbestic near 340 nm defining the entire time course. For *RpaETF*, early changes differ from those later in the photoreduction (Figure 3B).

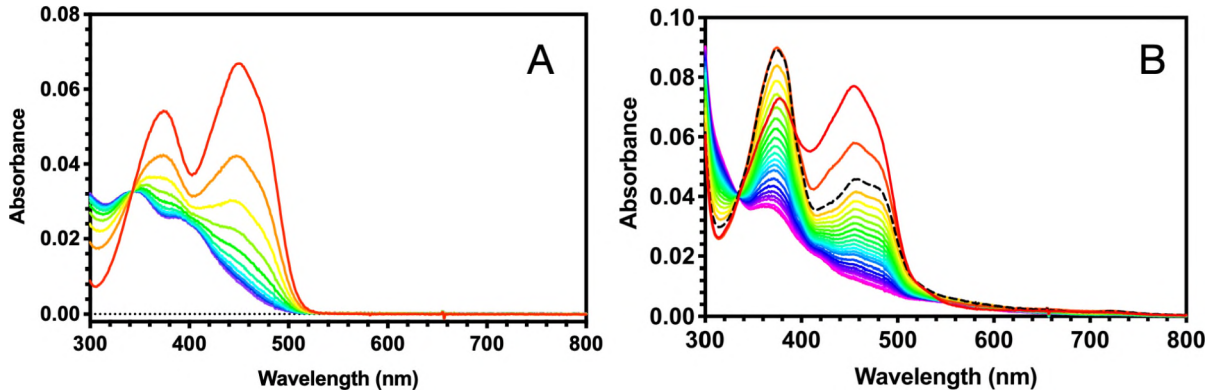


Figure 3: comparison of stages of photoreduction of free FAD in Tris buffer (A), vs *RpaETF* in BTP buffer (B). In order to slow the course of photoreduction of free FAD the reaction was conducted in Tris buffer (A), whereas for *RpaETF* BTP buffer was used (B), and inert atmosphere was used throughout except where stated otherwise. The buffer was 20 mM Tris or BTP, pH 9.0, 200 mM KCl, 10% (w/v) glycerol, and WT *RpaETF* was 14.4 μ M. Spectra were collected via a 2 mm path length while under blue light (450 nm) illumination via the perpendicular 1 cm path length of the cuvette. Spectra in panel A were recorded at time intervals of 0.25 min. and some photodamage is evident at the end. Spectra in panel B were monitored at time intervals of 0.25 min from 0 min to 3.5 min, then at time intervals of 0.5 min from 3.5 min to 6 min, finally at time intervals of 1 min from 6 min to 8 min. The initial spectra are in red and the last ones are in pink. For *RpaETF*, the maximal ASQ population observed at 0.5 min is indicated by the black dashed line. Negligible changes occurred after 8 min, although data were collected through 11 min.

In photoreductions of protein-bound flavins, initial formation of ASQ is generally considered to result from internal electron transfer to the photoexcited flavin from a near-by electron-donating amino acid side chain [45]. However, the resulting side chain cation radical can undergo rapid recombination that reoxidizes the flavin [46, 47]. This would tend to decrease the yield of ASQ observed in experiments such as ours, lacking short-time resolution. We will only observe longer-lived products that accumulate, for example, if electron donation from BTP to photo-oxidized side chains prevents their recombination with flavin ASQ, or if BTP is itself the electron donor to the flavin as for free FAD. The much slower flavin reduction observed in *RpaETF* than for free FAD shows that the protein greatly diminishes FAD's photoreactivity overall, possibly by diminishing its access to BTP. In a second contrast with free FAD, photoreduction of *RpaETF* reveals accumulation of ASQ as an intermediate. On thermodynamic grounds this is expected to stem from the ET-flavin alone [13, 48]. To test this, we compared photoreduction with equilibrium chemical reduction because the latter produces the ASQ of the ET-flavin, ET-ASQ.

Clues to the identity of the photogenerated ASQ – The photochemical formation and then further reduction of ASQ bore superficial resemblance to the effects of stepwise reduction with dithionite under equilibrium conditions (Supporting Fig. 1A, B). However photoreduction was characterized by two phases only (Figure 4A), whereas equilibrium titrations with dithionite displayed three distinct phases (Figure 4B). The three phases of equilibrium chemical reduction have been identified as initial formation and then consumption of ET-ASQ [13], followed by reduction of Bf-OX to Bf-HQ (Bf-flavin OX state to HQ state, Fig. 4B). The three-phase behavior was observed in published reductive titrations using NADH, sodium dithionite, or the xanthine/xanthine oxidase system [10, 11, 15, 49, 50]. While the nature of phase 1 of photoreduction resembled that of phase I of chemical reduction (blue traces in panels 4C and 4D), the spectral changes late in photoreduction were different from those late in equilibrium chemical reduction

(red difference spectra in Fig. 4 C vs. D). The spectral changes late in photoreduction were dominated by reduction of ASQ to HQ [13]. The presence of a clean isosbestic near 334 nm argues that photoreduction phase 2 does not comprise two overlapping but chemically distinct stages (Figure 5 inset).

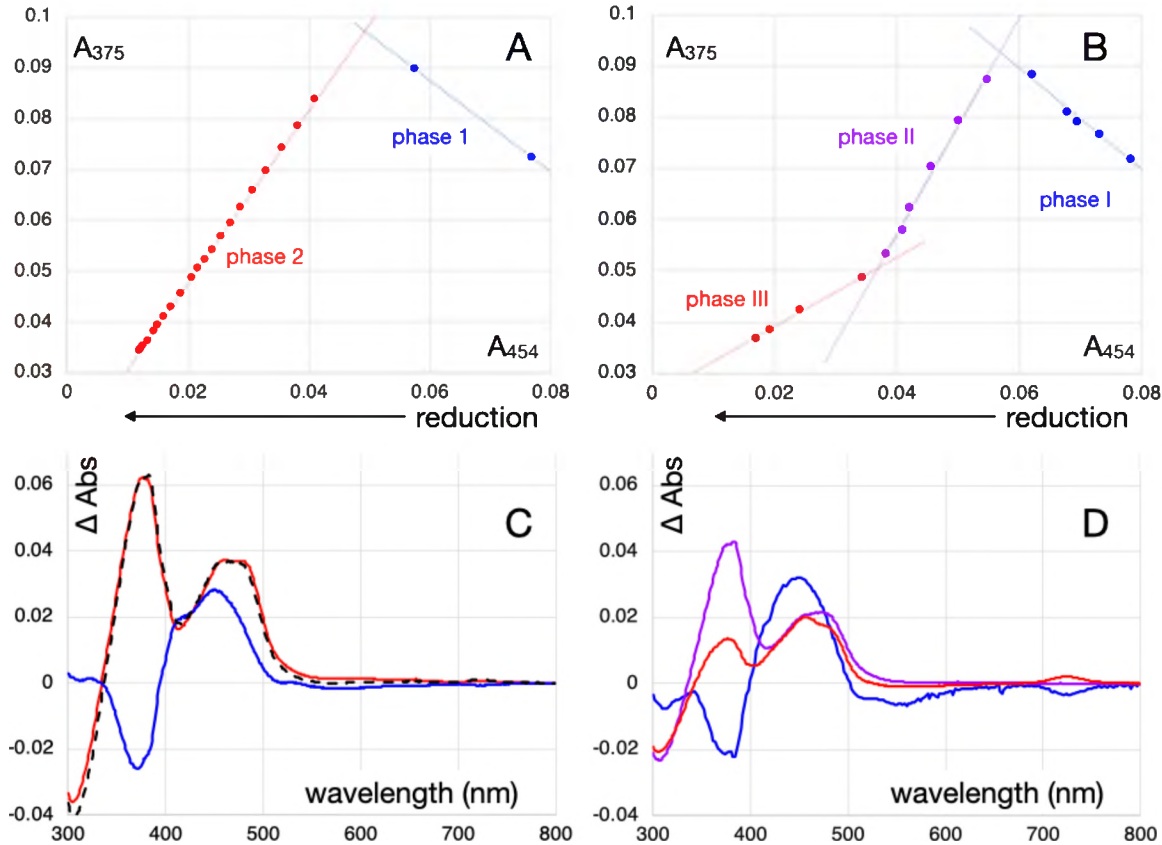


Fig. 4. Comparison of the course of photoreduction (A, C) vs. chemical reduction (B, D) of WT *RpaETF*. A, B: Ratio of intensity in band II (375 nm) to that in band I (455 nm), as a function of duration of illumination (A) or extent of chemical reduction (B). The data in (A) derive from the reduction described in Figure 3B. The reductive titration (B, D) involved reduction of 400 μ L WT protein (14.4 μ M) by 0.82 mM sodium dithionite in 20 mM BTP, pH 9.0, 200 mM KCl, 10% (w/v) glycerol, monitored with a 2 mm path length. Data points reflect the following added volumes of dithionite: 2 μ L, 3.5 μ L, 5.5 μ L, 6.5 μ L, 10 μ L, 12 μ L, 14 μ L, 16 μ L, 17 μ L, 18 μ L, 19 μ L, 24 μ L, 26 μ L, 28 μ L. C, D: Difference spectra corresponding to the first point in each phase minus the last one in the course of photoreduction (C) and chemical reduction (D). For C, the difference spectrum corresponding to the first phase was obtained as the spectrum at 0 min minus that at 0.25 min scaled to $\Delta A_{375} = -0.025$ to depict the full first-point-to-intersection amplitude of the phase. For the second phase it was the spectrum at 0.75 min. minus that at 8 min scaled to a ΔA_{375} of 0.062 to depict this interval's full amplitude from intersection to end-point. For D, the difference spectrum corresponding to the first phase was obtained as the spectrum after 0 additions of dithionite minus that at 5 scaled to $\Delta A_{375} = -0.021$ to depict the full first-point-to-intersection amplitude of the phase, for the second phase it was the spectrum after 5 additions minus that after 11 scaled to $\Delta A_{375} = 0.0422$ to depict the full intersection-to-intersection amplitude of the phase, and for the third phase it was the spectrum after 12 additions minus that after 15 scaled to a ΔA_{375} of 0.0136 to depict this interval's full amplitude from intersection to end-point. For details and derivations of the scaling factors, please see the supporting information Figures S2 describing the analysis of the equilibrium chemical reductive titration and S3 describing the analysis of the photoreduction.

Additionally, the maximum photo-accumulation of ASQ was larger than in the case of thermodynamic titrations. The amplitude of the last phase of photoreduction suggests that some 1.3 ASQ equivalents accumulate in the *RpaETF* during sustained illumination at pH 9.0 (red curve in Fig. 4C), based on comparison with the maximal yield of ASQ in equilibrium titrations (purple in Fig. 4D, and for details see

the supporting information related to Fig. S3) [48]. The estimated steady-state population well below 2 flavin equivalents is consistent with the mechanistic proposal that Bf-ASQ is highly unstable [16] and observations that Bf-ASQ does not accumulate in equilibrium titrations [10, 11, 15, 49, 51].

We also characterized the photogenerated ASQ regarding the rates of formation and further reaction. In the second phase of photoreduction, absorbance at 375 nm can be fit with a single exponential decay yielding a rate constant k_d of 0.45 min^{-1} corresponding to a 1.6 min half time (Figure 5). This is much slower than the rate of formation estimated at $k_f \approx 9 \text{ min}^{-1}$, assuming simple sequential formation and then consumption of ASQ (Figures 5 and 3B). These rate constants and the model yield that maximal ASQ is expected at 0.35 min, consistent with our data. At this time, the model indicates that 80% of the competent sites assume the ASQ state (details in Supporting Information accompanying Fig. S4). Thus our observed signal amplitude corresponding to ≈ 1.3 flavins per ETF invokes participation of 1.6 flavins per ETF, which is readily accommodated by our flavin content of 2 per dimer (Supporting Table S1).

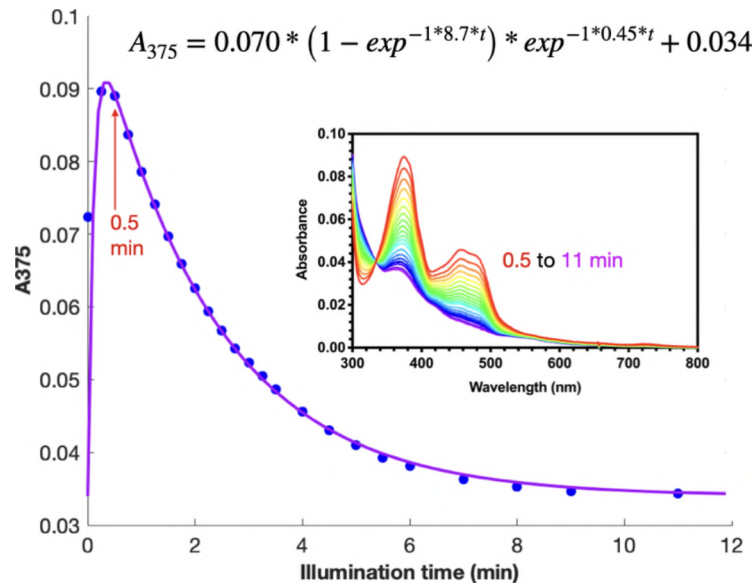


Fig. 5. Formation and consumption of ASQ as indicated by absorbance at 375 nm, and modeled by exponential growth and decay. The inset shows spectra collected from 0.5 minutes onward, showing the isosbestic indicative of a homogeneous second phase of photoreduction of WT *Rpa*ETF in BTP under blue light illumination. The spectrum obtained at 0.5 min is in red and spectra characterizing later time points run through purple. These are drawn from the anaerobic photoreduction of $14.4 \mu\text{M}$ WT protein described in Fig. 3B. The expression for exponential growth and decay with parameters that best fit the data is shown. These observations can be attributed to bound flavin only, on the basis of the contrasting kinetics vs. those observed for free FAD.

The foregoing employs the simplification of considering that both flavins are subject to the same rate constants, due to our limited time resolution. Comparable rates are likely applicable for the rate of photoproduction of ASQ from OX, based on the very high energy per photon of 2.75 eV (450 nm) which greatly exceeds even the largest estimate of the energy required to drive formation of Bf-ASQ, of $E^{\circ}_{\text{OX/ASQ}} = 0.9 \text{ V}$ [9]. The rate of disappearance of Bf-ASQ is expected to be much faster than that of ET-ASQ [9, 15, 52], but if a population of Bf-ASQ dissipates via an ET-ASQ intermediate then both processes could be subject to the same rate-limiting step, which our experiments would detect. If such a process occurs, it implies that one flavin can obtain electrons via the other.

Photostimulation of internal electron transfer – To assess the possible significance of electron transfer between *Rpa*ETF's two flavins, we illuminated *Rpa*ETF in which the ET site was pre-reduced to the HQ state using dithionite, but the Bf-flavin remained OX (ET-HQ/Bf-OX). In such samples, only the Bf-flavin has significant light-absorbing capacity at 450 nm so primary photochemistry should be restricted

to that site. Thus the simplest expectation is that any ASQ formed should represent the Bf-site. However if excited Bf-flavin acquires an electron from the ET-HQ, that will produce ET-ASQ in addition to Bf-ASQ. Thus, up to half of the total ASQ formed could represent ET-ASQ, but the other half of initially observed ASQ should correspond to Bf-ASQ.

There was clear immediate production of ASQ (Fig. 6A). The speed with which ASQ developed was roughly twice that observed in samples in which both flavins were OX (Fig. 6C). This is consistent with the fact that two reducing equivalents were already present at the ET site, and indicates that internal electron transfer to the Bf site was faster than acquisition of electrons from solution. Extended illumination of such half-reduced samples accomplished full reduction with spectral changes resembling those of the second phase of photoreduction of the fully oxidized *Rpa*ETF, including an isosbestic point at 334 nm (Fig. 6A, vs. 5 inset). However full reduction was achieved slightly earlier in samples that were half-reduced to start with, than in samples beginning fully OX (Fig. 6A inset).

The fast initial formation of ASQ suggests that reduction of Bf-OX to ASQ draws on electrons at the ET-HQ. Thus we infer that ASQ is generated at both sites, at least transiently. This is consistent with the more rapid photoreduction of ASQ observed in this case, with $k_d=0.56\text{ min}^{-1}$, than for ASQ formed in *Rpa*ETF that started in its ET-OX/Bf-OX state (tabulated in supporting information Table S2). The faster reaction of ASQ in the half-reduced case is consistent with a greater contribution from less stable Bf-ASQ.

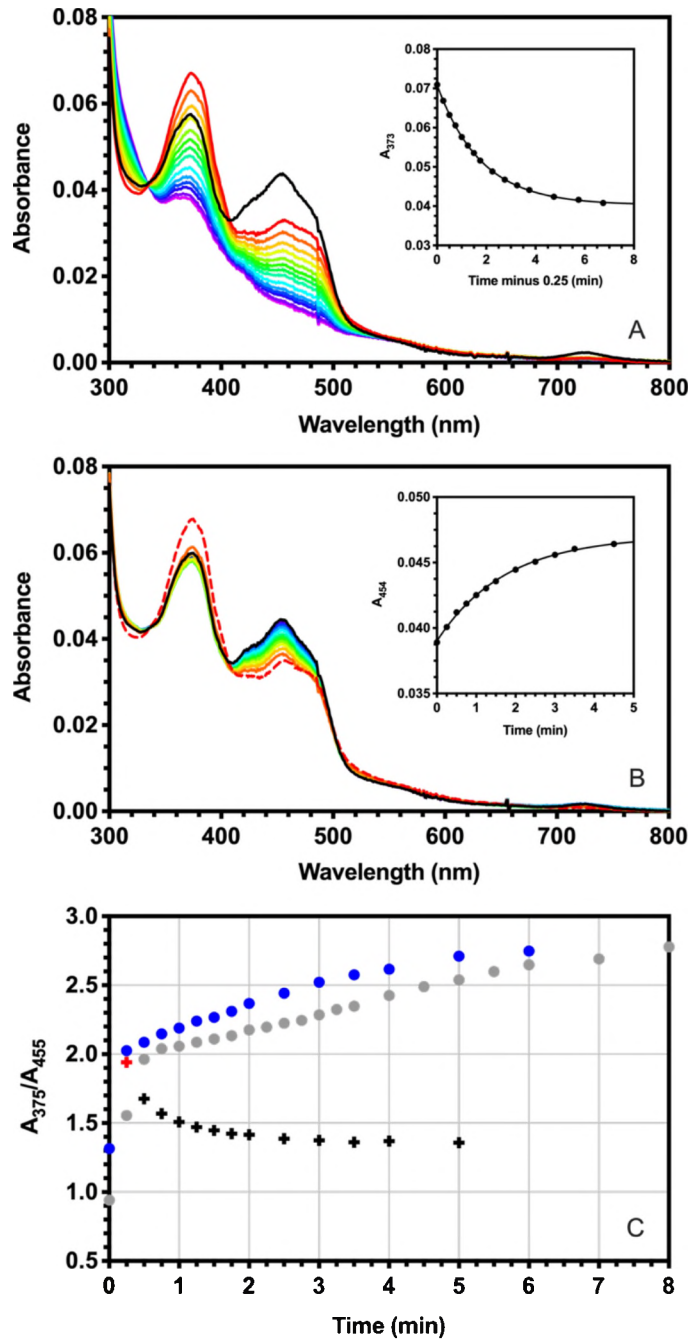


Fig. 6. Photoreduction of half-reduced WT *RpaETF*. (A) Time course of anaerobic photoreduction of 14.4 μM WT protein that was pre-reduced halfway by dithionite, in 20 mM BTP, pH 9.0, 200 mM KCl, 10% (w/v) glycerol, monitored with a 2 mm path length under blue light (450 nm) illumination. Spectra were monitored at time intervals of 0.25 min from 0 min to 2 min, then at time intervals of 0.5 min from 2 min to 4 min, finally at time intervals of 1 min from 4 min to 6 min (red to purple). The initial spectrum is shown in black. Inset shows amplitude of 373 nm band as a function of time after 0.25 min. Amplitudes were fit to a single exponential decay in time yielding $y = 0.040 + 0.031 e^{-0.56t}$, where t is time in minutes since 0.25 min. (B) Time course of equilibration of 14.4 μM WT protein that was pre-reduced halfway by dithionite, then briefly illuminated (≤ 1 sec.) with blue light (450 nm) in 20 mM BTP, pH 9.0, 200 mM KCl, 10% (w/v) glycerol, and then monitored with a 2 mm path length. Spectra were monitored at time intervals of 0.25 min from 0 min to 1.5 min, then at time intervals of 0.5 min from 1.5 min to 3.5

min, finally at time intervals of 1 min from 3.5 min to 4.5 min (red through blue). The initial dark state spectrum is shown in solid black and the spectrum produced upon brief illumination is shown in dashed red (time point zero). Inset shows amplitude of 454 nm band as a function of time after cessation of illumination. Amplitudes were fit to a single exponential growth function, $y = 0.039 + 0.008 (1 - e^{-0.57t})$, where t is time in minutes. (C) Ratio of intensity of band II to band I as a function of time, comparing the response to continuous illumination beginning from a completely oxidized state (grey, Fig. 3B data) to the response of a sample prepared in the ET-HQ/Bf- OX state (blue, data from panel A) and the equilibration after brief (≤ 1 sec.) illumination of a sample prepared as ET-HQ/Bf- OX (crosses, data from panel B; the red cross indicates the ratio immediately upon illumination and the black crosses chart its evolution during equilibration in darkness).

To explicitly test for redistribution of labile electrons among the flavins on the time scale of the experiment, and to address the stability of the ET-ASQ/Bf-ASQ state proposed to participate above, we reproduced the early portion of the experiment, using brief illumination of *Rpa*ETF that had been half reduced by dithionite, to generate ASQ (≤ 1 sec.). As shown in Fig. 6B, the sample returned to its pre-illumination distribution of reducing equivalents indicating that no additional reducing equivalents were acquired from the BTP on the time scale of the brief illumination, or during the dark period that followed it. Thus all transient spectral changes can be interpreted in terms of redistribution of an unchanged quantity of reducing equivalents. Consequently, the clear formation of ASQ observed upon brief illumination reflects comproportionation and must involve formation of Bf-ASQ as well as ET-ASQ, however briefly. The recovery in darkness confirms electron transfer between the flavins, this time from the transient Bf-ASQ to the ET-ASQ formed in parallel, to restore Bf-OX/ET-HQ (immediate drop in amplitude at 375 nm with little net change at 454 nm). After this burst phase, the starting spectrum was recovered with a slower rate constant of 0.57 min^{-1} and a difference spectrum that we attribute to redistribution of reducing equivalents among the two flavins, since these have distinct OX spectra [10, 53]. The instantaneous reversal of a substantial fraction of the photogenerated ASQ further confirms that the photo-generated ASQ included a contribution from Bf-ASQ. The immediate collapse of ASQ upon cessation of illumination (6B) also emphasizes the importance of continuous photoproduction in sustaining the steady-state ASQ levels reported in Figure 4.

Reduction of a low-potential electron acceptor: chemical evidence for formation of Bf-ASQ – To test for participation of Bf-ASQ in the ASQ population observed, we exploited the considerably lower E° of the OX/ASQ couple of Bf-flavin, compared to that of ET-flavin. Thus, although neither reduced state of the ET-flavin can reduce benzyl viologen (BV, $E^\circ = -374 \text{ mV}$ [54]), Wang et al have shown that the Bf-ASQ can do so [36]. Therefore we used reduction of BV as an assay for presence of Bf-ASQ. ASQ was generated as in Fig. 3B, but in the presence of BV. As demonstrated in Fig. 7, reduction of BV occurred, indicating that the ASQ observed included a contribution from Bf-ASQ.

The rate of BV reduction displayed a lag time of 0.75 min, similar to the time required for formation of maximal ASQ (Figures 7B and 5). At 5.5 min, 27 μM of BV had been reduced. Some of this was caused by the deuterium lamp used to collect spectra, as a control experiment without *Rpa*ETF yielded 6 μM BV of photoreduced BV^\cdot (Supporting Fig. S5A). BV^\cdot continued to accumulate for longer, but data collected to 5.5 minutes sufficed to document reduction of 21 μM BV in excess of the 14 mM concentration of *Rpa*ETF, and thus catalytic reduction of this low- E° carrier.

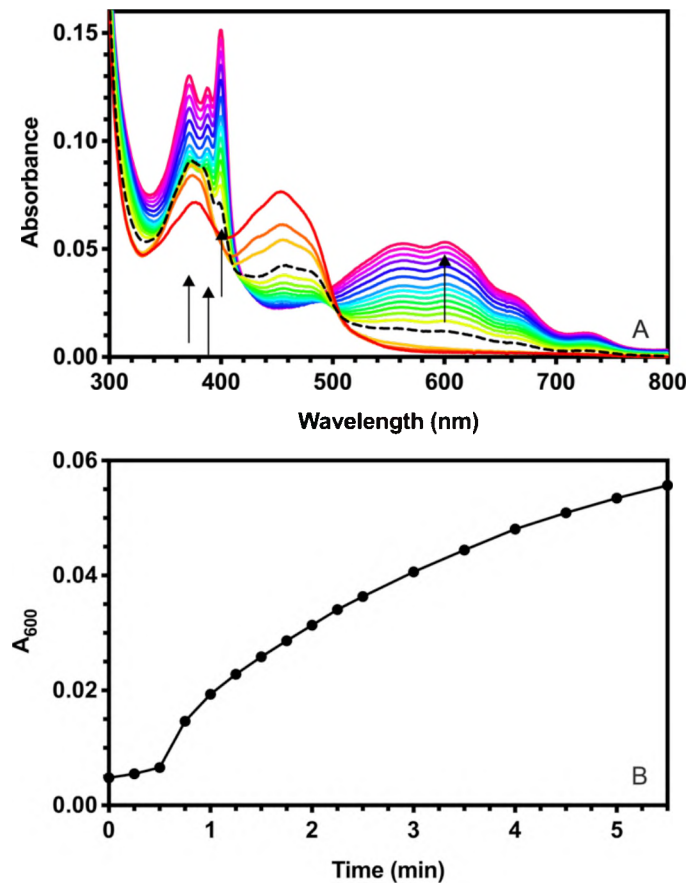


Fig. 7. Reduction of benzyl viologen (BV) by Bf-ASQ. (A) UV-visible spectra of 14.4 μ M WT *RpaETF* in the presence of 149.6 μ M BV in 20 mM BTP, pH 9.0, 200 mM KCl, 10% (w/v) glycerol, monitored with a 2 mm path length under blue light (450 nm) illumination. Spectra were monitored at time intervals of 0.25 min from 0 min to 2.5 min, then at time intervals of 0.5 min from 2.5 min to 5.5 min (red to pink). The maximal ASQ formation was shown in dashed black. Sharp lines near 380 nm accompanied by increased intensity between 500 to 750 nm reveal formation of reduced BV^+ . (B) Time course of reduction of BV monitored at 600 nm; maximal Bf-ASQ accumulation was observed at 0.75 min. Lines between dots are provided simply to guide the eye.

Lifetime of photogenerated ASQ is extended in variant C174A.L – Conventional wisdom is that the immediate electron donor to a photoexcited flavin would be a nearby amino acid side chain [45-47], and that external donors would react more slowly or re-reduce oxidized amino acids. Given that both tyrosine and cysteine residues are able to donate an electron, and participate in the photocycle of flavoprotein blue light receptors [55-59], we investigated the role of two conserved residues, Tyr-37.S and Cys-174.L, 4 \AA from ET-flavin and Bf-flavin, respectively. These are the closest electron-rich side chains to the flavins, with the next closest ones being another Cys 6 \AA from the Bf-flavin and then a Tyr 7.5 \AA from the ET-flavin (no Trps are within 10 \AA). Variants Y37F.S and C174A.L accumulated yields of ASQ on par with WT under the same conditions (Fig. 8A and S7A), although accumulation was slightly slower (0.75 min required to achieve maximum yield in variants). Conversion of ASQ to HQ by continued photoreduction was similar in nature and speed to WT, for the Y37F.S variant (half-time of 1.5 min, Fig. S7A). In contrast, photoreduction of ASQ in C174A.L was more sluggish (Fig. 8A, $t_{1/2} = 2.4$ min) implicating Cys-174.L in the second phase of flavin reduction.

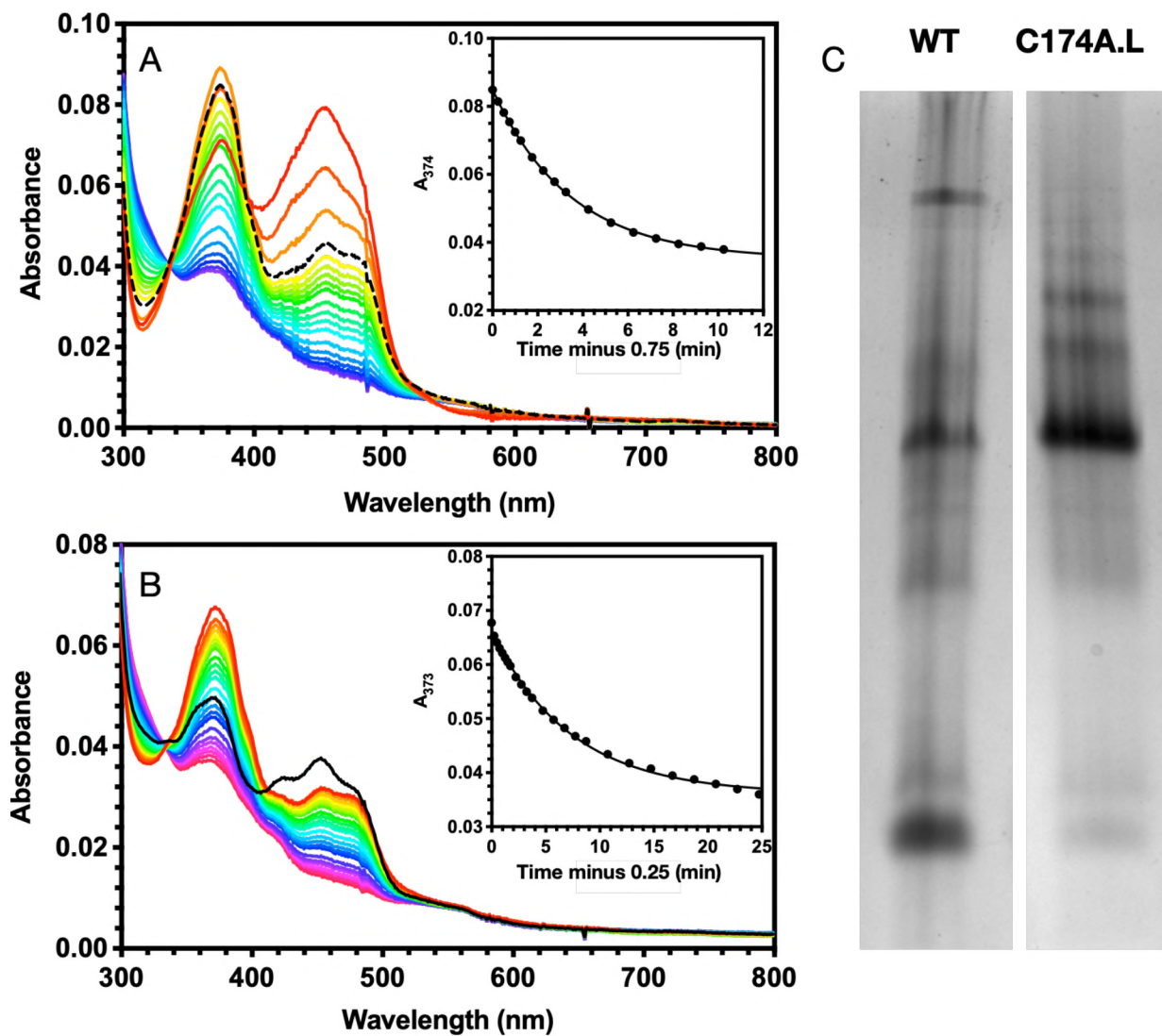


Fig. 8. (A) Time course of anaerobic photoreduction of 14.4 μ M C174A.L in 20 mM BTP, pH 9.0, 200 mM KCl, 10% (w/v) glycerol, monitored with a 2 mm path length under blue light (450 nm) illumination. Spectra were monitored at time intervals of 0.25 min from 0 min to 2 min, then at time intervals of 0.5 min from 2 min to 4 min, finally at time intervals of 1 min from 4 min to 10 min (red to blue). The maximal ASQ population observed at 0.75 min is indicated by the black dashed line. Inset shows amplitude of 374 nm band as a function of time starting from maximal ASQ formation at 0.75 min. Amplitudes were fit to a single exponential decay in time, $y = 0.035 + 0.050 e^{-0.29t}$, where t is time in minutes after 0.75 min, yielding a half-life of 2.4 min in C174A.L vs. the 1.6 min obtained for WT. (B) Time course of anaerobic photoreduction of 14.4 μ M C174A.L that was pre-reduced halfway by dithionite, in 20 mM BTP, pH 9.0, 200 mM KCl, 10% (w/v) glycerol, monitored with a 2 mm path length under blue light (450 nm) illumination. Spectra were monitored at time intervals of 0.25 min from 0 min to 2 min, then at time intervals of 0.5 min from 2 min to 4 min, then at time intervals of 1 min from 4 min to 9 min, finally at time intervals of 2 min from 9 min to 23 min (red to pink). The initial spectrum is shown in black. Inset shows amplitude of 373 nm band as a function of time starting from maximal ASQ formation at 0.25 min. Amplitudes were fit to a single exponential decay in time, $y = 0.036 + 0.030 e^{-0.14t}$, where t is time in minutes since 0.25 min, yielding a half-life of 5.1 min, vs the WT value of 1.2 min. (C) Blue Native gel of WT and C174A.L run at 4 °C in the dark. A predominantly “compact” or more anionic protein conformation was observed for WT, in contrast, C174A.L adopted almost exclusively a retarded “expanded” or less anionic protein conformation [60].

When Y37F.S or C174A.L variants were prepared in the ET-HQ/Bf-OX state via chemical reduction by dithionite and then illuminated with blue light, an immediate shift from ET-HQ/Bf-OX to ET-ASQ/Bf-ASQ was observed as in WT (Fig. 8B and Fig. S7B), confirming electron transfer between the two flavins. Nevertheless, ensuing photoreduction of photogenerated ASQ was substantially slower for the variants, especially C174A.L, whose half-life was longer than its WT counterpart (5.1 min, Fig. 8B). One possibility is that in WT, anionic Cys-174.L acts as a proximal electron donor to the Bf-ASQ and thereby accelerates electron delivery. Alternately or in addition, it could provide a proton. However the modest (four-fold) change in rate argues against a change in mechanism, in favor of more subtle modulation of the process, for example via perturbation of the populations of conformations present in solution. So far, the three conformations captured crystallographically and by cryoelectron microscopy place the two flavins at very different distances from one another, and vary the solvent exposure of the ET-flavin [12, 61, 62]. Indeed, WT and C174A.L displayed distinct populations of protein conformations in blue native PAGE analysis (Fig. 8C). Whereas the same conformations were observed in both cases, arguing against disruption of structure by the C174A.L substitution, the faster-migrating (more compact and/or negatively charged) conformation dominated for WT whereas a retarded (expanded and/or less anionic) conformation was dominant for C174A.L.

Discussion

A highly reducing semiquinone state of the Bf-flavin is considered to be a key requirement for flavin-based electron bifurcation [3, 4, 9]. Such a species was proposed to participate in the catalytic cycle of the EtfABCX from *Pyrobaculum aerophilum* upon transient formation of ET-HQ/Bf-ASQ from ET-ASQ/Bf-HQ [11]. We have updated a traditional use of flavin photochemistry to enable steady-state accumulation of flavin ASQ [41-43], including some 0.3 equivalents of Bf-ASQ. While the presence of two flavins complicates quantification of the ASQ attributable to Bf-ASQ, several lines of evidence converge on the interpretation that Bf-ASQ contributes. These are (1) the considerably larger difference spectrum associated with ASQ formed under photochemical reduction vs. equilibrium chemical titration, (2) immediate formation of ASQ upon illumination of ET-HQ/Bf-OX *Rpa*ETF without acquisition of electrons from solution, (3) immediate disappearance of a substantial fraction of ASQ upon cessation of illumination despite the relative stability of ET-ASQ and (4) ability of illuminated *Rpa*ETF to reduce BV but only after the time required to form ASQ, despite the inability of ET-ASQ to reduce BV. These data support that the population of ASQ observed under steady-state illumination at pH 9 includes some from the Bf site.

We attribute the steady-state population of Bf-ASQ to our use of high pH and blue light. Blue light stimulates formation of the excited state of OX flavin, which in turn abstracts an electron to form ASQ [45, 63, 64]. However further photoreduction requires proton acquisition, whereas our use of a pH above the pK_a of 8.3 of flavin SQ disfavors this, and thus any advance beyond ASQ. Thus we propose that rate-limiting proton acquisition is responsible for the slowness of the second phase of photoreduction, as well as its greater sensitivity to mutation of Cys-174.L. Cys-174 could aid in proton transfer to N5, as observed in some LOV domains [65, 66]. For any sites that do acquire a proton, the resulting NSQ requires 350 and 560 nm light for optimal photoreduction, not the 450 ± 10 nm light emitted by our diode [67-69]. In contrast, traditional photochemical experiments employed white light, which efficiently drives both reductions [29, 41]. Thus our experiment incorporates two features that favor accumulation of ASQ rather than full reduction to HQ.

Ours and other work demonstrates that Bf-ASQ reacts rapidly [15, 52], so the Bf-ASQ steady-state population indicated here is most likely possible only due to continuous production of flavin ASQ via blue-light illumination. We confirmed the thermodynamic instability of the ET-ASQ/Bf-ASQ state by demonstrating its immediate conversion to ET-HQ/Bf-OX upon cessation of blue light illumination (Fig. 6). Our use of an efficient sacrificial electron donor also forestalled chemical damage during the

sustained illumination required to build up detectable Bf-ASQ. Our observation of Bf-ASQ is moreover consistent with several literature examples in which photoreduction (catalyzed by free flavin) results in population of a SQ state that is not thermodynamically stable [29, 43, 70].

Additional requirements for bifurcation include two efficient, divergent paths of electron transfer [9]. Thus it is significant that the current work demonstrates functional flavin-to-flavin electron transfer within the ETF, which had previously been suggested by a spectroscopic signature [48], and hinted at by results attributed at the time to inter-ETF electron transfer [49], but has now been reported based on direct kinetic measurements while the current paper was undergoing review [52]. Given that NADH is a two-electron donor while the ET-flavin of ETF mediates one-electron reactivity [13, 15, 49], it is believed that NADH reduces Bf-flavin [10-13] and internal electron transfer from Bf-HQ to ET-ASQ, generates ET-HQ along with a transient, highly-reactive, Bf-ASQ [10, 12, 13, 52]. Here we provide further evidence of the required internal electron transfer between the two flavins, in both directions: immediately upon illumination of half-reduced *Rpa*ETF, photoexcited Bf-OX acquired an electron from ET-HQ to form ET-ASQ/Bf-ASQ (Fig. 6A, Fig. 8B and Fig. S7B), and the reverse was evident when illumination was stopped at the ET-ASQ/Bf-ASQ stage and the sample returned to the ET-HQ/Bf-OX state (Fig. 6B). While the initial reduction of Bf-OX in the presence of ET-HQ could in-principle have occurred via electron capture from BTP, that would have increased the number of reducing equivalents present in *Rpa*ETF. However we employed a very brief illumination that did not result in acquisition of reducing equivalents from solution, as shown by the system's return to an ET-HQ/Bf-OX state indistinguishable from that before illumination. Thus during the brief illumination, internal electron transfer outpaced electron acquisition from the medium.

The functional relevance of any Bf-ASQ formed is supported by *Rpa*ETF's ability to mediate light-driven reduction of BV based on BTP. NfnI has been shown to mediate NADH-based reduction of BV as a model Bf reaction [36]. Herein we used continuous irradiation with blue light to sustain a population of ASQ able to reduce BV, and therefore attributed to the Bf-flavin. This validates a critical component of the accepted mechanism of flavin-based bifurcation.

Photoreduction of ETFs has been reported for several canonical ETFs, but in these cases free deazaflavin served as the photo-catalyst along with sacrificial electron donors such as EDTA [71-73]. In the current study, we determined that our BTP buffer could serve as the electron donor. This is consistent with seminal work by Frisell *et al.* showing that deprotonated alkyl amines are good electron donors to photoexcited flavin, even if they lack a carboxylate functionality [40]. Given BTP's two secondary amines with pK_{as} of 6.8 and 9.0 *vs.* our solution pH of 9, our finding is, indeed, expected. Since BTP also supports photoreduction of free flavin in aqueous solution (Fig. 2B), our application of BTP can potentially be extended to other flavoproteins as well. This will be particularly valuable in cases when deazaflavin use is not possible. Our finding also raises a cautionary note, that in studies of flavoenzymes employing amine buffers and not protecting the enzyme from light, under-appreciated light-driven photoreduction of the flavin could contribute to the results.

The strong protective effect of BTP recalls the crucial role of the protein environment in providing rescuing or passivating residues to pre-empt damaging photochemistry, for example in flavodoxins and dodecins [74, 75]. Of the 4 tryptophan and 13 tyrosine residues in *Rpa*ETF, only Tyr-37.S approaches within 5 Å of a flavin, and that affects only the ET-flavin in the B-like conformation [10]. This is consistent with relatively inefficient internal quenching of *Rpa*ETF's flavins, and thus *Rpa*ETF's capacity to mediate net light-driven reactions of substrates in solution, such as BTP or BV. Another structural factor of likely significance is that both of *Rpa*ETF's flavins appear significantly exposed to solvent with solvent accessible surface area for the isoalloxazine ring as high as 50 Å² *vs.* the 240 Å² total area of the isoalloxazine ring, (Supporting Fig. S6, [10, 12, 13]) consistent with the reactivity of Bf-flavin with dissolved O₂ [51]. The structure of EtfABCX from *Thermotoga maritima* indicates that the ET-flavin is much less exposed in the complex [62], and it is expected that upon association of the low- E° acceptor ferredoxin or flavodoxin, the Bf-flavin will also be sequestered in a protein-protein interface [12].

The slower photoreduction of flavin ASQ to HQ in C174A.L is interesting. A conserved Cys residue in the LOV domains (light, oxygen voltage) reductively adds to the flavin ring at C4a upon

photoexcitation of the flavin (reviewed in [21]). The Cys-174.L in *RpaETF* is closer to the flavin C6 position, where a cysteinyl adduct is formed in histamine dehydrogenase [76] and trimethylamine dehydrogenase [77]. The 6-S-Cys flavin adduct in histamine dehydrogenase has an absorbance centered at 440 nm and the flavin precipitates with the protein upon protein denaturation, neither of which are true in our case. Therefore, we do not suspect formation of a 6-S-Cys adduct with Cys-174 in *RpaETF*. Additionally, the E° s of C174.L-*RpaETF* are very similar to those of the WT protein [48], so we do not attribute the slower photoreduction of ASQ to HQ to a more difficult reduction. Instead, the slower conversion of ASQ to HQ in C174A.L may reflect a protein conformation shift (Fig. 8C), which could affect access of BTP to the flavins, in addition to the inter-flavin distance. Residue Cys-174.L is conserved as Cys among diazotrophs, but not Bf-ETFs in general [32]. This raises the intriguing possibility of a regulatory or protective role for Cys-174.L.

Tyrosine side chains can be sources of an electron and a proton for photoexcited flavins, as documented in BLUF (blue light sensing using FAD) domains [37, 78], glucose oxidase [79] and flavodoxin [45, 64]. However substitution of Tyr-37.S with Phe did not greatly affect photoreduction of the ET-OX/Bf-OX or ET-HQ/Bf-OX states, suggesting that Tyr-37.S is not required for photoreduction or inter-flavin electron transfer, although it is 4.2 Å from the ET flavin in the B-like conformation, and Tyr side chains can mediate electron hopping (Supporting Figure S7) [80]. The fact that mutations do modulate the rates associated with photo reduction strengthen the interpretation that we are observing bound, not free FAD. Similarly the greater effect of mutating C174.L buried near the Bf-flavin, than Ty37.S on the surface near the ET-flavin, indicates that our kinetics contain a contribution from the Bf-flavin.

Finally, the current work demonstrates the capacity of light to drive reduction of Bf-flavin to its HQ state. Meanwhile, we and others have already demonstrated Bf-HQ's ability to reduce NAD⁺ to NADH [11, 81]. Thus, the current work provides the missing link to complete a demonstration that Bf-ETF can be used to mediate light-driven formation of a long-lived stable closed-shell chemical fuel molecule: NADH. This work confirms central mechanistic premises of flavin-based electron bifurcation and sets the stage for detailed time-resolved studies employing absorbance and fluorescence, which are essential in order to arbitrate on open questions including proton acquisition by the flavins, the fate of the electron donor, and possible involvement of amino acids and the adenines of the FADs.

Materials and Methods

Protein purification of R. palustris ETF and its variants - Generation of a construct for the expression of WT *RpaETF*, site-directed mutagenesis for producing Y37F.S and C174A.L variants and protein expression were described elsewhere [48]. Protein purification was also carried out as previously [48] but with a modified FAD reconstitution method to minimize the time protein was exposed to pH 9 buffers. Instead of removing imidazole first and then reconstituting protein with FAD at pH 9 overnight, the pooled pure fractions from the Ni-nitrilotriacetic acid column were reconstituted with FAD immediately by incubation of the protein in 1 mM FAD, 20 mM Tris, pH 7.8, 500 mM KCl at 4 °C in darkness for 30 min. Imidazole and excess flavin were then removed by gel filtration on a 10DG column (Bio-Rad Laboratories, Hercules, CA) and the protein was buffer-exchanged into 20 mM BTP, pH 9.0, 200 mM KCl, 10% (w/v) glycerol before prompt use or flash-freezing in liquid nitrogen and storage at -80 °C.

Flavin content quantification – Protein concentration was determined using the Pierce 660 nm protein assay (Thermo Fisher Scientific, Waltham, MA). To quantify the flavin content, the protein sample was denatured in 10 mM cetyltrimethylammonium bromide (CTAB) at room temperature in the dark for 5 min [48]. The concentration of FAD was then quantified spectrophotometrically using the extinction coefficient $\epsilon_{450} = 11.3 \text{ mM}^{-1} \text{ cm}^{-1}$ [82] and correcting for dilution due to addition of 44.4 μL of 100 mM CTAB stock solution to 400 μL of a protein sample.

Photochemistry – Protein samples of WT, Y37F.S or C174A.L were made anaerobic and used at a final concentration of 14.4 μM in 400 μL. Anaerobic photoreduction was performed on a HP 8453 diode

array spectrophotometer (Agilent Technologies, Santa Clara, CA) using a 2 mm path length fluorescence quartz cuvette sealed with an airtight screw cap (Starna Cells, Atascadero, CA) in 20 mM BTP, pH 9.0, 200 mM KCl, 10% (w/v) glycerol. A 450 nm 10 W LED spot light source with an aluminum heatsink housing ('Royal Blue' LEDSupply, Randolph, VT) was used to illuminate the center of the sample with the beam perpendicular to the path of the spectrophotometer's light path (1 cm path length), at a distance of 25 cm from the side wall of the cuvette. 450 nm photons have energy corresponding to 2.76 eV. For photoreduction of the half-reduced protein, titration with dithionite was first carried out in a HP 8452A spectrophotometer (Agilent Technologies, Santa Clara, CA) equipped with an Olis controller (Bogart, GA) housed in a Belle Technology (Weymouth, United Kingdom) glovebox (<1.8 ppm of oxygen) to achieve the half-reduced state, then the resulting sample was illuminated with blue light and monitored as described above. The decay of photogenerated ASQ, i.e., reduction of ASQ to HQ, monitored at 374 ± 1 nm over time, was fit into a single exponential decay model:

$$y = y_{\min} + (y_0 - y_{\min}) e^{-kt},$$

where y_0 is the initial A_{374} , y_{\min} is the infinite-time A_{374} asymptote, t is time and k is the rate constant.

The data in panel 6B were fit according to single exponential growth:

$$y = y_0 + (y_{\max} - y_0)(1 - e^{-kt}),$$

where y_0 is the initial value, k is the rate constant, t is the time, and y_{\max} is the infinite-time asymptote).

To describe exponential growth and decay together, as in Figure 5, we fit the data with

$$A_{375} = \Delta A_{\text{tot}}(1 - e^{k_f t})(e^{-k_d t}) + A_{\text{offset}}$$

where ΔA_{tot} is the total change in A_{375} and A_{offset} is the infinite-time asymptote, k_f and k_d are the rate constants for formation and decay of absorbance at 375 nm. To calculate the time at which A_{375} would attain its maximum value, the derivative with respect to time was equated to zero and solved obtain the optimum time. Using that we could calculate the maximum value of the population of ASQ, p_{ASQ} , as a function of the total starting population able to form it, p_{ox} , as follows

$$p_{\text{ASQ}} = p_{\text{ox}}(1 - e^{k_f t})(e^{-k_d t}) .$$

Reduction of BV by WT *RpaETF* was accomplished by inclusion of 149.6 μM BV in the photoreduction and BV radical was quantified using an extinction coefficient of $10.4 \text{ mM}^{-1} \text{ cm}^{-1}$ at 600 nm [83].

Blue Native PAGE – Protein conformations of WT and C174A.L were evaluated by Blue Native PAGE [60] using a 4-20% Mini-PROTEAN® TGXTM precast polyacrylamide gradient gel (Bio-Rad Laboratories, Hercules, CA) run at 4 °C in darkness. Protein bands were visualized by Coomassie blue G-250 and imaged using a ChemiDoc MP Imaging System (Bio-Rad Laboratories, Hercules, CA). Protein bands were excised and the presence of both ETF subunits was verified by mass spectrometry (data not shown).

Flavin solvent accessible surface areas – Solvent accessible surface areas (SASareas) were calculated on a per-atom basis using the default parameters of Chimera, and the areas of atoms in the isoalloxazine ring were summed [84]. H atoms were not added.

Acknowledgements

HDD was supported by the National Sciences Foundation, Chemistry of Life Processes CHE-1808433. SAK was supported by the U.S. Department of Energy, Office of Science, Office of Basic Energy Sciences under Award Number DE-SC0021283 as well as EPSCoR PON2 635 2000003148. The authors declare that they have no conflicts of interest with the contents of this article.

References

- [1] W. Buckel, R.K. Thauer, ‘Flavin-based electron bifurcation, a new mechanism of biological energy coupling.’, *Chem. Rev.*, 118 (2018).
- [2] V. Müller, N.P. Chowdhury, M. Basen, ‘Electron bifurcation: A long-hidden energy-coupling mechanism’, *Annu. Rev. Microbiol.*, 72 (2018) 331-353.
- [3] W. Nitschke, M.J. Russell, ‘Redox bifurcations: Mechanisms and importance to life now, and at its origin.’, *Bioessays*, 34 (2012) 106-109.
- [4] J.W. Peters, A.F. Miller, A.K. Jones, P.W. King, M.W. Adams, ‘Electron bifurcation’, *Curr. Opin. Chem. Biol.*, 31 (2016) 146–152.
- [5] G. Herrmann, E. Jayamani, G. Mai, W. Buckel, ‘Energy conservation via electron-transferring flavoprotein in anaerobic bacteria’, *J. Bacteriol.*, 190 (2008) 784-791.
- [6] F. Baymann, B. Schoepp-Cothenet, S. Duval, M. Guiral, M. Brugna, C. Baffert, M.J. Russell, W. Nitschke, ‘On the natural history of flavin-based electron bifurcation’, *Frontiers in Microbiology*, 9 (2018) 1357.
- [7] J.W. Peters, D.N. Beratan, B. Bothner, R.B. Dyer, C.S. Harwood, Z.M. Heiden, R. Hille, A.K. Jones, P.W. King, Y. Lu, C.E. Lubner, S.D. Minteer, D.W. Mulder, S. Raugei, S.G. J., L.C. Seefeldt, M. Tokmina-Lukaszewska, O.A. Zadvornyy, P. Zhang, M.W.W. Adams, ‘A new era for electron bifurcation’, *Curr. Opin. Chem. Biol.*, 47 (2018) 32-38.
- [8] J.L. Yuly, C.E. Lubner, P. Zhang, D.N. Beratan, J.W. Peters, ‘Electron bifurcation: progress and grand challenges.’, *Chem. Commun.*, 55 (2019).
- [9] C.E. Lubner, D.P. Jennings, D.W. Mulder, G.J. Schut, O.A. Zadvornyy, J.P. Hoben, M. Tokmina-Lukaszewska, L. Berry, D.M. Nguyen, G.L. Lipscomb, B. Bothner, A.K. Jones, A.F. Miller, P.W. King, M.W.W. Adams, J.W. Peters, ‘Mechanistic insights into energy conservation by flavin-based electron bifurcation’, *Nat Chem Biol*, 13 (2017) 655-659.
- [10] N.P. Chowdhury, A.M. Mowafy, J.K. Demmer, V. Upadhyay, S. Koelzer, E. Jayamani, J. Kahnt, M. Hornung, U. Demmer, U. Ermler, W. Buckel, ‘Studies on the Mechanism of Electron Bifurcation Catalyzed by Electron Transferring Flavoprotein (Etf) and Butyryl-CoA Dehydrogenase (Bcd) of *Acidaminococcus fermentans*.’, *J. Biol. Chem.*, 289 (2014) 5145-5157.
- [11] G.J. Schut, N.R. Mohamed-Raseek, M. Tokmina-Lukaszewska, D.E. Mulder, D.M.N. Nguyen, G.L. Lipscomb, J.P. Hoben, A. Patterson, C.E. Lubner, P.W. King, J.W. Peters, B. Bothner, A.F. Miller, M.W.W. Adams, ‘The catalytic mechanism of electron bifurcating electron transfer flavoproteins (ETFs) involves an intermediary complex with NAD⁺.’, *J. Biol. Chem.*, 294 (2019) 3271-3283.
- [12] J.K. Demmer, N.P. Chowdhury, T. Selmer, U. Ermler, W. Buckel, ‘The semiquinone swing in the bifurcating electron transferring flavoprotein/butyryl-coA dehydrogenase complex from *Clostridium difficile*.’, *Nat. Commun.*, 8 (2017) 1577.
- [13] N. Mohamed-Raseek, H.D. Duan, M.A. Mroginski, A.F. Miller, ‘Spectroscopic, thermodynamic and computational evidence of the locations of the FADs in the nitrogen fixation-associated electron transfer flavoprotein.’, *Chemical Sci.*, 10 (2019) 7762-7772.
- [14] W. Nitschke, M.J. Russell, ‘Redox bifurcations: mechanisms and importance to life now, and at its origin: a widespread means of energy conversion in biology unfolds...’, *Bioessays*, 34 (2012) 106-109.
- [15] H.D. Duan, C.E. Lubner, M. Tokmina-Lukaszewska, G.H. Gauss, B. Bothner, P.W. King, J.W. Peters, A.F. Miller, ‘Distinct flavin properties underlie flavin-based electron bifurcation within a novel electron-transferring flavoprotein FixAB from *Rhodopseudomonas palustris*’, *J. Biol. Chem.*, 293 (2018) 4688-4701.

[16] J.P. Hoben, C.E. Lubner, M.W. Ratzloff, G.J. Schut, D.M.N. Nguyen, K.W. Hempel, M.W.W. Adams, P.W. King, A.F. Miller, 'Equilibrium and ultrafast kinetic studies manipulating electron transfer: A short-lived flavin semiquinone is not sufficient for electron bifurcation', *J Biol Chem*, 292 (2017) 14039-14049.

[17] R.N. Ledbetter, A.M. Garcia Costas, C.E. Lubner, D.E. Mulder, M. Tokmina-Lukaszewska, J.H. Artz, A. Patterson, T.S. Magnuson, Z.J. Jay, H.D. Duan, J. Miller, M.H. Plunkett, J.P. Hoben, B.M. Barney, R.P. Carlson, A.-F. Miller, B. Bothner, P.W. King, J.W. Peters, L.C. Seefeldt, 'The Electron Bifurcating FixABCX Protein Complex from *Azotobacter vinelandii*: Generation of Low-Potential Reducing Equivalents for Nitrogenase Catalysis', *Biochemistry*, 56 (2017) 4177-4190.

[18] S.J.O. Hardman, C.R. Pudney, S. Hay, N.S. Scrutton, 'Excited state dynamics can be used to probe donor-acceptor distances for H-tunneling reactions catalized by flavoproteins.', *Biophys. J.*, 105 (2013) 2549-2558.

[19] J.M. Robbins, J. Geng, B.A. Barry, G. Gadda, A.S. Bommarius, 'Photoirradiation generates an ultrastable 8-formyl FAD semiquinone radical with unusual properties in formate oxidase.', *Biochemistry*, 57 (2018) 5818-5826.

[20] I. Chaves, R. Pokorny, M. Byrdin, N. Hoang, T. Ritz, K. Brettel, L.O. Essen, G.T. van der Horst, A. Batschauer, M. Ahmad, 'The cryptochromes: blue light photoreceptors in plants and animals', *Annu. Rev. Plant Biol.*, 62 (2011) 335-364.

[21] K.S. Conrad, C.C. Manahan, B.R. Crane, 'Photochemistry of flavoprotein light sensors.', *Nat. Chem. Biol.*, 10 (2014) 801-809.

[22] J. Herrou, S. Crosson, 'Structure, function and mechanism of bacterial photosensory LOV proteins.', *Nat. Rev. Microbiol.*, 9 (2011) 713-723.

[23] A. Losi, W. Gärtner, 'Old chromophores, new photoactivation paradigms, trendy applications: flavins in blue light-sensing photoreceptors.', *Photochem. Photobiol.*, 87 (2011) 491-510.

[24] A. Losi, W. Gärtner, 'The evolution of flavin-binding photoreceptors: an ancient chromophore serving trendy blue-light sensors', *Annu. Rev. Plant Biol.*, 63 (2012) 49-72.

[25] A. Sancar, 'Structure and function of DNA photolyase and cryptochrome blue-light photoreceptors.', *Chem. Rev.*, 103 (2003) 2203-2237.

[26] B.D. Zoltowski, K.H. Gardner, 'Tripping the light fantastic: blue-light photoreceptors as examples of environmentally modulated protein-protein interactions.', *Biochemistry*, 50 (2011) 4-16.

[27] D. Su, C. Smitherman, G. Gadda, 'A metastable photoinduced protein-flavin adduct in choline oxidase, an enzyme not involved in light-dependent processes.', *J. Phys. Chem. B*, 124 (2020) 3936-3943.

[28] V. Massey, P. Hemmerich, 'Photoreduction of flavoproteins and other biological compounds catalyzed by deazaflavins.', *Biochemistry*, 17 (1978) 9-16.

[29] V. Massey, M.T. Stankovich, P. Hemmerich, 'Light-mediated reduction of flavoproteins with flavins as catalysts.', *Biochem.*, 17 (1978) 1-8.

[30] S.-H. Song, B. Dick, A. Penzkofer, 'Photo-induced reduction of flavin mononucleotide in aqueous solutions', *Chem. Phys.*, 332 (2007) 55-65.

[31] P.F. Heelis, 'The photophysical and photochemical properties of flavins (isoalloxazines)', *Chem. Soc. Rev.*, 11 (1982) 15-39.

[32] A.M. Garcia Costas, S. Poudel, A.-F. Miller, S.G. J., R.N. Ledbetter, K. Fixen, L.C. Seefeldt, M.W. Adams, C.S. Harwood, E.S. Boyd, J.W. Peters, 'Defining Electron Bifurcation in the Electron Transferring Flavoprotein Family', *J. Bacteriol.*, (2017).

[33] T. Edgren, S. Nordlund, 'The fixABCX genes in *Rhodospirillum rubrum* encode a putative membrane complex participating in electron transfer to nitrogenase.', *J. Bacteriol.*, 186 (2004) 2052–2060.

[34] A. Lukacs, R.-K. Zhao, A. Haigney, R. Brust, G.M. Greetham, M. Towrie, P.J. Tonge, S.R. Meech, 'Excited state structure and dynamics of the neutral and anionic flavin radical revealed by ultrafast transient mid-IR to visible spectroscopy.', *J. Phys. Chem. B.*, 116 (2012) 5810-5818.

[35] M. Tilo, I.H.M. van Stokkum, C. Bonetti, P. Hegemann, J.T.M. Kennis, 'The Hydrogen-Bond Switch Reaction of the Blrb Bluf Domain of *Rhodobacter sphaeroides* .', *J. Phys. Chem. B.*, 115 (2011) 24.

[36] S. Wang, H. Huang, J. Moll, R.K. Thauer, 'NADP⁺ reduction with reduced ferredoxin and NADP⁺ reduction with NADH are coupled via an electron-bifurcating enzyme complex in *Clostridium kluyveri* .', *J. Bacteriol.*, 192 (2010) 5115-5123.

[37] M. Gauden, J.S. Grinstead, W. Laan, I.H.M. van Stokkum, M. Avila-Perez, K.C. Toh, R. Boelens, R. Kaptein, R. van Grondelle, K.J. Hellingwerf, J.T.M. Kennis, 'On the role of aromatic side chains in the photoactivation of BLUF domains', *Biochemistry*, 46 (2007) 7405-7415.

[38] F. Cailliez, P. Müller, T. Firmino, P. Pernot, A. de la Lande, 'Energetics of photoinduced charge migration within the tryptophan tetrad of an animal (6-4) photolyase.', *J. Am. Chem. Soc.*, 138 (2016) 1904-1915.

[39] T. Biskup, E. Schleicher, A. Okafuji, G. Link, K. Hitomi, E.D. Getzoff, S. Weber, 'Direct observation of a photoinduced radical pair a cryptochrome blue-light photoreceptor.', *Angew. Chem. Int. Ed.*, 48 (2009) 404-407.

[40] W.R. Frisell, C.W. Chung, C.G. Mackenzie, 'Catalysis of oxidation of nitrogen compounds by flavin coenzymes in the presence of light." ', *J. Biol. Chem.*, 234 (1959) 1297-1302.

[41] V. Massey, G.A. Palmer, 'On the existence of spectrally distinct classes of flavoprotein semiquinones. A new method for the quantitative production of flavoprotein semiquinones.', *Biochem.*, 5 (1966) 3181-3189.

[42] G. Nöll, G. Hauska, P. Hegemann, K. Lanzl, T. Nöll, M. von Sanden-Flohe, B. Dick, 'Redox Properties of LOV Domains: Chemical versus Photochemical Reduction, and Influence on the Photocycle', *Chem. Bio. Chem.*, 8 (2007) 2256-2264.

[43] M.T. Stankovich, L.M. Schopfer, V. Massey, 'Determination of glucose oxidase oxidation-reduction potentials and the oxygen reactivity of fully reduced and semiquinoid forms', *J Biol Chem*, 253 (1978) 4971-4979.

[44] W. Holzer, J. Shirdel, P. Zirak, A. Penzkofer, P. Hegemann, R. Deutzmann, E. Hochmuth, 'Photo-induced degradation of some flavins in aqueous solution.', *Chem. Phys.*, 308 (2005) 69-78.

[45] D.P. Zhong, A.H. Zewail, 'Femtosecond dynamics of flavoproteins: charge separation and recombination in riboflavin (vitamin B-2)-binding protein and in glucose oxidase enzyme', *Proc. Natl. Acad. Sci. U.S.A.*, 98 (2001) 11867-11872.

[46] R.L. Martin, F. Lacombat, A. Espagne, N. Dozova, P. Plaza, J. Yamamoto, P. Müller, K. Brettel, A. de la Lande, 'Ultrafast flavin photoreduction in an oxidized animal (6-4) photolyase through an unconventional tryptophan tetrad.', *Phys. Chem. Chem. Phys.*, 19 (2017) 24493-24504.

[47] Z. Liu, C.Y. Tan, X. Guo, J. Li, L. Wang, A. Sancar, D. Zhong, 'Determining complete electron flow in the cofactor photoreduction of oxidized photolyase.', Proc Natl Acad Sci U S A, 110 (2013) 12966-12971.

[48] H.D. Duan, N. Mohamed-Raseek, A.F. Miller, 'Spectroscopic evidence for direct flavin-flavin contact in a bifurcating electron transfer flavoprotein.', J. Biol. Chem., 295 (2020) 12618-12634.

[49] K. Sato, Y. Nishina, K. Shiga, 'Interaction between NADH and electron-transferring flavoprotein from *Megasphaera elsdenii*', J. Biochem., 153 (2013) 565-572.

[50] J. Sucharitakul, S. Buttranon, T. Wongnate, N.P. Chowdhury, M. Prongjit, W. Buckel, P. Chaiyen, 'Modulations of the reduction potentials of flavin-based electron bifurcation complexes and semiquinone stabilities are key to control directional electron flow.', FEBS J., ASAP (2020) doi:10.1111/febs.15343.

[51] N.P. Chowdhury, J. Kahnt, W. Buckel, 'Reduction of ferredoxin or oxygen by flavin-based electron bifurcation in *Megasphaera elsdenii*', FEBS J., 282 (2015) 3149-3160.

[52] J. Sucharitakul, W. Buckel, P. Chaiyen, 'Rapid kinetics reveal surprising flavin chemistry in the bifurcating electron transfer flavoprotein from *Acidaminococcus fermentans*', J. Biol. Chem., ASAP (2020).

[53] K. Sato, Y. Nishina, K. Shiga, 'Purification of electron-transferring flavoprotein from *Megasphaera elsdenii* and binding of additional FAD with an unusual absorption spectrum', J. Biochem, 134 (2003) 719-729.

[54] P. Wardman, 'The reduction potential of benzyl viologen: an important reference compound for oxidant/radical redox couples.', Free Rad. Res. Commun., 14 (1991) 57-67.

[55] M.T.A. Alexandre, T. Domratcheva, C. Bonetti, L.J. van Wilderen, R. van Grondelle, M.L. Groot, K.J. Hellingwerf, J.T.M. Kennis, 'Primary reactions of the LOV2 domain of phototropin studied with ultrafast mid-infrared spectroscopy and quantum chemistry.', Biophys. J., 97 (2009) 227-237.

[56] P. Goyal, S. Hammes-Schiffer, 'Role of active site conformational changes in photocycle activation of the AppA BLUF photoreceptor.', Proc. Natl. Acad. Sci. U S A, 114 (2017) 1480-1485.

[57] D. Holub, H. Ma, N. Krauß, T. Lamparter, M. Elstner, N. Gillet, 'Functional role of an unusual tyrosine residue in the electron transfer chain of a prokaryotic (6-4) photolyase.', Chem. Sci., 9 (2018) 1259-1272.

[58] A. Pfeifer, T. Majerus, M.K. Zikihara, D. Matsuoka, S. Tokutomi, J. Heberle, T. Kottke, 'Time-resolved Fourier transform infrared study on photoadduct formation and secondary structural changes within the phototropin LOV domain.', Biophys. J., 96 (2009) 1462-1470.

[59] J.P. Zayner, T.R. Sosnick, 'Factors that control the chemistry of the LOV domain photocycle.', PLoS One, 9 (2014) e87084.

[60] G.J. Fiala, W.W. Schamel, B. Blumenthal, 'Blue native polyacrylamide gel electrophoresis (BN-PAGE) for analysis of multiprotein complexes from cellular lysates.', J. Vis. Exp., (2011) doi: 10.3791/2164.

[61] H.S. Toogood, D. Leys, N.S. Scrutton, 'Dynamics driving function : new insights from electron transferring flavoproteins and partner complexes.', FEBS J., 274 (2007) 5481-5504.

[62] X. Feng, G.J. Schut, G. Lipscomb, H.Y. Li, M.W.W. Adams, 'Cryoelectron microscopy structure and mechanism of the membrane-associated electron-bifurcating flavoprotein Fix/EtfABCX.', Proc Natl Acad Sci U S A, 118 (2021) e2016978118.

[63] N. Hoang, E. Schleicher, S. Kacprzak, J.-P. Bouly, M. Picot, W. Wu, A. Berndt, E. Wolf, R. Bittl, M. Ahmad, 'Human and *Drosophila* Cryptochromes Are Light Activated by Flavin Photoreduction in Living Cells', *PLOS Biol.*, 6 (2008) e200.

[64] N. Mataga, H. Chosrowjan, S. Taniguchi, F. Tanaka, N. Kido, M. Kitamura, 'Femtosecond fluorescence dynamics of flavoproteins: comparative studies on flavodoxin, its site-directed mutants, and riboflavin binding protein regarding ultrafast electron transfer in protein nanospaces.', *J. Phys. Chem. B.*, 106 (2002) 8917-8920.

[65] C.E. Bauer, C.-R. Rabl, J. Heberle, T. Kottke, 'Indication for a radical intermediate preceding the signaling state in the LOV domain photocycle.', *Photochem. Photobiol.*, 87 (2011) 548-553.

[66] B.D. Zoltowski, B. Vaccaro, B.R. Crane, 'Mechanism-based tuning of a LOV domain photoreceptor.', *Nature, Chem. Biol.*, 5 (2009) 827-834.

[67] J.-P. Bouly, E. Schleicher, M. Dionisio-Sese, F. Vandenbussche, D. van der Straeten, N. Bakrim, S. Meier, A. Batschauer, P. Galland, R. Bittl, M. Ahmad, 'Cryptochrome Blue Light Photoreceptors Are Activated through Interconversion of Flavin Redox States', *J. Biol. Chem.*, 282 (2007) 9383-9391.

[68] J. Pan, M. Byrdin, C. Aubert, A.P.M. Eker, K. Brettel, M.H. Vos, 'Excited-state properties of flavin radicals in flavoproteins: femtosecond spectroscopy of DNA photolyase, glucose oxidase, and flavodoxin.', *J. Phys. Chem. B*, 108 (2004) 10160-10167.

[69] M. Byrdin, A. Lukacs, V. Thiagarajan, A.P.M. Eker, K. Brettel, M.H. Vos, 'Quantum yield measurements of short-lived photoactivation intermediates in DNA photolyase: toward a detailed understanding of the triple tryptophan electron transfer chain.', *J. Phys. Chem. A*, 114 (2010) 3207-3214.

[70] P. Augustin, A. Hromic, T. Pavkov-Keller, K. Gruber, P. Macheroux, 'Structure and biochemical properties of recombinant human dimethylglycine dehydrogenase and comparison to the disease-related H109R variant.', *FEBS J.*, 283 (2016) 3587-3603.

[71] P. Augustin, M. Toplak, K. Fuchs, E.C. Gerstmann, R. Prassl, A. Winkler, P. Macheroux, 'Oxidation of the FAD cofactor to the 8-formyl-derivative in human electron-transferring flavoprotein.', *J. Biol. Chem.*, 293 (2018) 2829-2840.

[72] V.L. Davidson, M. Husain, J.W. Neher, 'Electron transfer flavoprotein from *Methylophilus methylotrophus*: properties, comparison with other electron transfer flavoproteins, and regulation of expression by carbon source.', *J. Bacteriol.*, 166 (1986) 812-817.

[73] M. Toplak, J. Brunner, C.R. Tabib, P. Macheroux, 'Closing the gap: yeast electron-transferring flavoprotein links the oxidation of d-lactate and d- α -hydroxyglutarate to energy production via the respiratory chain.', *FEBS J.*, 286 (2019) 3611-3628.

[74] R. Artali, G. Bombieri, F. Meneghetti, G. Gilardi, S.J. Sadeghi, D. Cavazzini, G.L. Rossi, 'Comparison of the refined crystal structures of wild-type (1.34 Å) flavodoxin from *Desulfovibrio vulgaris* and the S35C mutant (1.44 Å) at 100 K.', *Acta Crystallogr D Biol Crystallogr*, 58 (2002) 1787-1792.

[75] H. Staudt, D. Oesterhelt, M. Grininger, J. Wachtveitl, 'Ultrafast excited-state deactivation of flavins bound to dodecin.', *J. Biol. Chem.*, 287 (2012) 17637-17644.

[76] N. Fujieda, A. Satoh, N. Tsuse, K. Kano, T. Ikeda, '6-S-cysteinyl flavin mononucleotide-containing histamine dehydrogenase from *Nocardioides simplex*: Molecular cloning, sequencing, overexpression and characterization of redox centers of the enzyme.', *Biochem*, 43 (2004) 10800-10808.

[77] D.J. Steenkamp, W. McIntire, W.C. Kenney, 'Structure of the covalently bound coenzyme of trimethylamine dehydrogenase', *J. Biol. Chem.*, 253 (1978) 2818-2824.

[78] T. Mathes, I.H.M. van Stokkum, M. Stierl, J.T.M. Kennis, 'Redox modulation of flavin and tyrosine determines photoinduced proton-coupled electron transfer and photoactivation of BLUF photoreceptors.', *J. Biol. Chem.*, 287 (2012) 31725-31738.

[79] L. Nag, A. Lukacs, M.H. Vos, 'Short-lived radical intermediates in the photochemistry of glucose oxidase.', *Chem. Phys. Chem.*, 20 (2019) 1793-1798.

[80] H.B. Gray, J.R. Winkler, 'Hole hopping through tyrosine/tryptophan chains protects proteins from oxidative damage', *Proc Natl Acad Sci U S A*, 112 (2015) 10920-10925.

[81] H.D. Duan, A.-F. Miller, 'Photogeneration and reactivity of a bifurcating flavin anionic semiquinone in a bifurcating electron transfer flavoprotein.', *Biochim. Biophys. Acta*, submitted (2020).

[82] L.G. Whitby, 'A new method for preparing flavin-adenine dinucleotide', *The Biochemical journal*, 54 (1953) 437-442.

[83] J.K. Kristjansson, T.C. Hollocher, 'First practical assay for soluble nitrous oxide reductase of denitrifying bacteria and a partial kinetic characterization.', *J. Biol. Chem.*, 255 (1980) 704-707.

[84] E.F. Pettersen, T.D. Goddard, C.C. Huang, G.S. Couch, D.M. Greenblatt, E.C. Meng, T.E. Ferrin, 'UCSF Chimera - a visualization system for exploratory research and analysis.', *J. Comput. Chem.*, 25 (2004) 1605-1612.